Assessment of the lower limb soft tissue artefact at marker-cluster level with a high-density marker set during walking

Arnaud Barre, Rachid Aissaoui, Kamiar Aminian, Raphaël Dumas

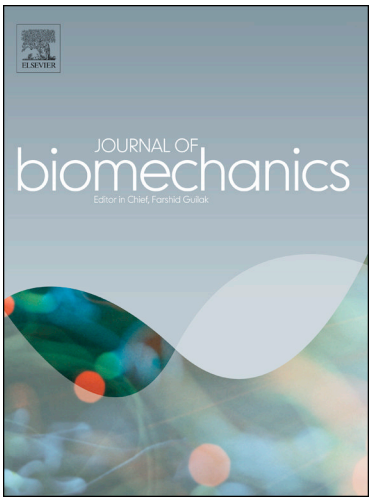

Assessment of the lower limb soft tissue artefact at marker-cluster level with a high-density marker set during walking

Arnaud Barré, Rachid Aissaoui, Kamiar Aminian, Raphaël Dumas

PII: S0021-9290(17)30254-3
DOI: http://dx.doi.org/10.1016/j.jbiomech.2017.04.036
Reference: BM 8222

To appear in: *Journal of Biomechanics*

Accepted Date: 30 April 2017

Please cite this article as: A. Barré, R. Aissaoui, K. Aminian, R. Dumas, Assessment of the lower limb soft tissue artefact at marker-cluster level with a high-density marker set during walking, *Journal of Biomechanics* (2017), doi: http://dx.doi.org/10.1016/j.jbiomech.2017.04.036

Assessment of the lower limb soft tissue artefact at marker-cluster level with a high-density marker set during walking

Arnaud Barré[1,2], Rachid Aissaoui[2], Kamiar Aminian[1], Raphaël Dumas[3,4],

[1] *Laboratory of Movement Analysis and Measurement, Ecole Polytechnique Fédérale de Lausanne, 1015 Lausanne, Switzerland*

[2] *Laboratoire de recherche en imagerie et orthopédie, Centre de recherche du Centre Universitaire Hospitalier de Montréal, École de technologie supérieure, Montréal, Canada.*

[3] *Univ Lyon, Université Claude Bernard Lyon 1, IFSTTAR, UMR_T9406, LBMC, F69622, Lyon, France*

[4] *Interuniversity Centre of Bioengineering of the Human Neuromusculoskeletal System, Università degli Studi di Roma "Foro Italico", Rome, Italy*

Word count: Abstract: 221, Main text: 2891

Abstract

The estimation of joint kinematics from skin markers is hindered by the soft tissue artefact (STA), a well-known phenomenon although not fully characterized. While most assessments of the STA have been performed based on the individual skin markers displacements, recent assessments were based on the marker-cluster geometrical transformations using, e.g., principal component or modal analysis. However, these marker-clusters were generally made of 4 to 6 markers and the current findings on the STA could have been biased by the limited number of skin makers analysed. The objective of the present study was therefore to confirm them with a high-density marker set, i.e. 40 markers placed on the segments.

A larger number of modes than found in the literature was required to describe the STA. Nevertheless, translations and rotations of the marker-cluster remained the main STA modes, archetypally the translation along the proximal-distal and anterior-posterior axes for the shank and the translation along the proximal-distal axis and the rotation about the medial-lateral axis for the thigh. High correlations were also found between the knee flexion angle and the amplitude of these modes for the thigh whereas moderate ones were found for the shank.

These findings support the current re-orientation of the STA compensation methods, from bone pose estimators which typically address the non-rigid components of the marker-cluster to kinematic-driven rigid-component STA models.

Keywords

Soft tissue artefact; rigid and non-rigid components; translation and rotation modes, knee joint angles, treadmill walking; total knee prosthesis

1. Introduction

Accurate estimation of the joint kinematics from skin markers is hindered by the well-known soft tissue artefact (STA): the relative displacement between the surface of the segments and the underlying skeleton. Numerous compensation methods have been proposed in the past which mainly addressed the deformation of the cluster of skin markers (Leardini et al., 2005). However, recent studies reported that the compensation methods should focus also on the rigid components of the STA (Benoit et al., 2015; Bonci et al., 2015; Camomilla et al., 2015; De Rosario et al., 2013; Dumas et al., 2015), that is to say the translations and rotations undergone by the marker-cluster.

Most studies which assessed the STA have been performed based on the individual skin markers displacements (Peters et al., 2010) and revealed that STA is segment, task, and subject-specific. More recent assessments were based on the marker-cluster geometrical transformations (Andersen et al., 2012; Benoit et al., 2015; Bonci et al., 2015; Dumas et al., 2014b; Grimpampi et al., 2013) using principal component analysis or modal analysis. Thus, it has been reported that (i) a limited number of modes could represent the STA (Andersen et al., 2012; Dumas et al., 2014b), that (ii) the rigid modes (i.e. translations and rotations of the marker-cluster) were generally main compared to the non-rigid modes (Benoit et al., 2015; de Rosario et al., 2012; Grimpampi et al., 2013), and that (iii) the rigid modes of the marker-cluster could be related to joint kinematics (Camomilla et al., 2015; Sangeux et al., 2006). These findings on the STA supported the statement that the bone pose estimators which typically address the deformation of the marker-cluster were unable to fully compensate for STA (Benoit et al., 2015; Bonci et al., 2015; Cappello et al., 2005; de Rosario et al., 2012; Dumas et al., 2015). These findings were the foundations of the development of different STA models (Andersen et al., 2012; Camomilla et

al., 2015; De Rosario et al., 2013; Richard et al., 2012). Nevertheless, the assessment based on the marker-cluster geometrical transformations was only performed, so far, on few subjects (from 3 to 10) and on markers-clusters generally made of 4 to 6 markers. It means that the number of possible modes to be analysed (i.e., *n* markers * 3 dimensions) remained limited. Typically, when *n* = 4, the number of possible modes matched the 12 modes defining the marker-cluster geometrical transformations (3 translations, 3 rotations, 3 streches, and 3 homotheties). In other words, these 12 modes always represented 100% of the STA energy (this energy stands for the displacements due to STA of all the skin markers). Therefore, it can be hypothesised that the recent focus on the rigid modes of the STA could have been biased by the limited number of skin makers analysed.

The objective of the present study was therefore to explore that, with a large number of markers placed on the segments, the aforementioned findings on the STA remains valid. The proposed study was based on retrospective data (Barré et al., 2015; Barré et al., 2013). This unique database, including 19 subjects with 40 skin markers placed on the thigh and shank, already revealed some marker-cluster rotation and translation similarities between subjects and few correlations with gait speed and body mass index. In the present study, all of the translations, rotations, homotheties, and stretches of the marker-cluster were analysed in terms of STA energy and correlations with the knee flexion angle.

2. Material and methods

2.1. STA assessment

This study is based on retrospective data obtained in 19 subjects (8 men, 11 women) with unilateral knee prosthesis (F.I.R.S.T, Symbios, CH) for at least one year (Barré et al., 2013). The mean±standard deviation of age, weight and height were 70±6 years, 80±14 kg, and 168±9 cm,

respectively. Subjects with symptomatic gait and pain were excluded. Briefly, the measurement systems consisted of two fluoroscopes (Philips, NL) coupled with a 7-camera optoelectronic system (Vicon, UK) during walking on a treadmill. From bi-plane fluoroscopic data, the knee prosthesis implanted onto the subject was registered in 3D with a sample frequency of 30Hz using Model-based RSA Software (RSAcore, NL). RMSE of 0.18^{o} is reported for the accuracy and precision of this registration (Barré et al., 2015). 80 semi-spherical reflective markers placed on the lower limb were tracked synchronously at 240 Hz. Each subject walked on the treadmill at a self-estimated comfortable speed (1.8±0.3 km/h) for 15 seconds. The reference frames of the prosthesis components were assumed to represent the anatomical frames of the femur and the tibia. For each component, the axes were defined as following: the X-axis is medial-lateral pointing to the left, the Y-axis is proximal-distal pointing upward, and the Z-axis is anterior-posterior pointing frontward. The assessment of the skin marker displacements due to the STA was computed as the relative movement of each raw marker coordinates with respect to a standing posture defined in a static trial and expressed in the femoral and tibial reference frames.

2.2. Modal representation of the STA

To assess the number of modes required to represent the STA, the proportion of rigid and non-rigid components, and the relation between maker-cluster geometrical transformations and joint kinematics, a modal representation of the STA was used. For that, the displacements that all skin markers undergo due to the STA were represented as an STA field, $\mathbf{V}$, which was approximated as a series of modes (a sum of time-dependant amplitudes, a, multiplied by constant basis vectors, $\mathbf{\Phi}$):

$$\mathbf{V}_i(k) \approx \sum_{l=1}^{12} \underbrace{\left(\mathbf{V}_i(k) \bullet \mathbf{\Phi}_i^l\right)}_{a_i^l(k)} \mathbf{\Phi}_i^l \quad , \tag{1}$$

where i stands for the segment (i = 1 for shank and i = 2 for thigh), k for the sampled instant of time (k = 1,…., n), and l for the mode (l = 1, …12). The first 6 modes describe the rigid components of the STA (3 translations and 3 rotations of the marker-cluster), while the 6 other modes describe the non-rigid components (3 homotheties and 3 stretches of the marker-cluster). The construction of these basis vectors, $\mathbf{\Phi}$, can be found in Dumas et al. (2014a). The amplitudes, a, were obtained by projection (dot product) of the STA field, $\mathbf{V}$, on the basis vectors, $\mathbf{\Phi}$ (Eq. 1).

The modes were ranked in a descending order according to their STA energy:

$$\lambda_i^l = \frac{1}{n} \sum_{k=1}^{n} \left(a_i^l(k)\right)^2 . \tag{2}$$

Only the first r_i modes that accounted for 80% of the STA total energy, e_i, were analysed:

$$\frac{\sum_{l=1}^{r_i} \lambda_i^l}{\underbrace{\frac{1}{n} \sum_{k=1}^{n} \left(\mathbf{V}_i(k)\right)^T \bullet \mathbf{V}_i(k)}_{e_i}} \geq 0.8 , \tag{3}$$

where $r_i \in (1,...,12)$ is the number of modes needed to account for $0.8e_i$.

Note that the maximal number of modes involved in the approximation of the STA field, $\mathbf{V}$, (r_i = 12) may eventually be not sufficient to account for 80% of e_i.

Thus, the number r_i represented directly the number of modes required to represent the STA while the ranking order indicated the proportion of rigid and non-rigid components. Then, the correlations between the amplitudes a_i^l and the knee flexion angle (Pearson's linear coefficient) were computed on the 15-second records for each of the 19 subjects. Only the correlations which

were statistically significant ($p < 0.05$) were analysed. Cross-correlations (i.e., time delay) were also computed to analyse the temporal relation between the amplitudes and the knee flexion angle. The correlations with the other knee joint angles were not investigated because, in an STA compensation perspective (i.e., in the absence of fluoroscopic measurements), these angles cannot be estimated accurately from skin markers. In the same way, the correlations for all 19 subjects pooled together were not computed because of the subject-specificity of STA.

3. Results

Concerning the number of modes required to represent the STA, for the shank, the number of modes $r_1 = 12$ was not sufficient to account for 80% of the STA total energy for 17 of the subjects out of the 19 (Table 1). For the thigh, the number of modes needed to account for 80% of the STA total energy was $r_2 \geq 6$ for one half of the subjects, i.e. 10 out of the 19 (Table 2).

As for the proportion of rigid and non-rigid components, for both shank and thigh, the translations and rotations appeared generally in the first ranked modes while the stretches and homotheties appeared in the last ranked modes. Some exceptions for the shank were the translation along the medial-lateral axis, the rotation about the medial-lateral and anterior-posterior axes (which appeared frequently in ranks #7 to #10), and the stretch about the proximal-distal axis (which appeared frequently in ranks #3 to #6). Similarly, two noticeable exceptions for the thigh were the rotation about the anterior-posterior axis (which appeared from time to time in ranks #7) and the stretch about the medial-lateral axis (which appeared frequently in ranks #3 to #6). Detailed results about the ranking orders are provided as Supplementary Material.

The amplitude of the translation along the shank proximal-distal axis (Figure 1A) was moderately correlated with the knee flexion angle. The mean and standard deviation of the correlation

coefficients for the 19 subjects were -0.522 ± 0.405. Conversely, the stretch and homothety about the proximal-distal axis (Figure 1B&C) were two modes for which the amplitudes were highly correlated with the knee flexion angle (0.727 ± 0.328 and 0.717 ± 0.263, respectively). For the thigh, the translation along the proximal-distal axis and the rotation about the medial-lateral axis (Figure 1D&E) were the two modes for which the amplitudes were highly correlated with the knee flexion angle (-0.845 ± 0.077 and 0.849 ± 0.145, respectively). The other correlation coefficients were all found below 0.5 except for the stretch about the proximal-distal axis of the thigh but for only 9 subjects out of the 19 (i.e., this mode was rarely required to represent the 80% of the STA total energy). Detailed results about the correlation coefficients are provided as Supplementary Material.

When analysing the temporal patterns of the amplitudes (Figure 1), except for the translation along the shank proximal-distal axis and the stretch and homothety about the same axis for three subjects, it did not appear that the heel strike event induced any specific shapes. Similarly, except for the stretch about the shank proximal-distal axis for two other subjects, the toe-off event did not induced any specific shapes. These five subjects were not characterised by any specific age, sex, BMI or walking speed.

As for the time delays between the amplitudes of the modes and the knee flexion angle, they demonstrated a very high variability across subjects. Logically, the lowest variabilities should be found for the aforementioned amplitudes for which the correlation with the knee flexion angle was high. Thus, the mean and standard deviation of the time delays for the 19 subjects were -0.120 ± 0.183 s for the translation along the shank proximal-distal axis, -0.072 ± 0.086 s and -0.066 ± 0.179 s for the stretch and homothety about the proximal-distal axis, respectively. For the thigh, the time delays were 0.042 ± 0.120 s and -0.003 ± 0.127 for the translation along the proximal-distal axis and the rotation about the medial-lateral axis, respectively. Detailed results

about the time delays are provided as Supplementary Material.

4. Discussion

The exploratory hypothesis of the present study was that the recent finding on the STA, focussed on the rigid modes, could have been biased by the limited number of skin makers analysed.

As a matter of fact, the number of modes that were required to account for 80% of the total STA energy was high: 12 modes for the shank for all the subjects but two as well as more than 6 modes for the thigh for half of the subjects. It seems that assessing STA with a large number of markers revealed a complex STA pattern, especially for the shank, that cannot be fully represented by the 12 geometrical transformations of the marker-cluster, conversely to what was previously reported with clusters generally made of 4 to 6 markers (Benoit et al., 2015; Dumas et al., 2014a, b). This result suggest the use of 3D interpolation and approximation methods rather than affine mapping (Dumas and Cheze, 2009) for the detailed representation of the STA.

Nonetheless, concerning the proportion of rigid and non-rigid components, translations and rotations appeared main with the clusters made of 40 markers, in agreement with what was previously reported with clusters made of 4 to 6 markers (Benoit et al., 2015; Dumas et al., 2014b; Grimpampi et al., 2013). In the present study, the translation along the proximal-distal and anterior-posterior axes for the shank, the translation along the proximal-distal axis and the rotation about the medial-lateral axis for the thigh accounted for the major part of the STA energy. However, the stretch energy about the proximal-distal axis for the shank and about the medial-lateral axis for the thigh was also present in the modes accounting for 80% of the STA total energy. Thus, the non-rigid component cannot be totally discarded if the displacements of the skin markers are to be considered as reported by Andersen et al. (2012). Furthermore, it is possible that bone pose estimators (Andriacchi et al., 1998; Dumas and Cheze, 2009; Heller et al.,

2011; Soderkvist and Wedin, 1993), which typically address the deformation of the STA, have an effect (however limited) on joint kinematics if a very large number of markers is used because the non-rigid components of the STA become substantial and because these components include other modes than stretch and homothety which have not been analysed so far (Bonci et al., 2015; Dumas et al., 2015). Though, the estimation of joint translations remains highly compromised because of the translation of the marker-cluster along the proximal-distal axis which appeared main for both shank and thigh. That is why multibody kinematics optimisation, which constraints the joint translations, has been instituted as a potential STA compensation method. Yet, the compensation effects, as assessed with different joint constraints, was still found limited (Richard et al., 2017).

Interestingly, correlations with the knee flexion angles were found for both rigid and non-rigid components: for the translation about the proximal-distal axis for both shank and thigh, for the rotation about the medial-lateral axis for the thigh, and for the stretch and homothety about the proximal-distal axis for the shank. As stated before, the number of modes required to account for 80% of the total STA energy was higher for the shank than for the thigh while the correlation for translation about the proximal-distal axis was lower for the shank than for the thigh. Moreover, different amplitude patterns were observed for the shank for some subjects, which were typically associated with the heel strike and toe-off events. It can be understood that the STA was more related to impacts and muscle contractions for the shank than for the thigh where the skin sliding may be predominant. Nevertheless, Akbarshashi et al. (2010) also reported sudden shifts of the thigh markers in the proximal direction immediately after heel strike that were not observed in the amplitudes of the translation of the marker-cluster of the thigh in the present study. Moreover, the analysis of the cross-correlations on the whole 15-second records revealed that the translation along the proximal-distal axis, which was a main STA mode, was leaded for the shank and

slightly lagged for the thigh with respect to the knee flexion angle. This analysis corroborated the idea that STA could be more related to impacts and muscle contractions for the shank than for the thigh.

Note that, to the best of the authors' knowledge, it is the first time that correlations and cross-correlations were established between marker-cluster geometrical transformations and joint angles. Up to now, similar correlations were established only for the individual skin displacements (Akbarshahi et al., 2010; Cappozzo et al., 1996; Fiorentino et al., 2016; Hara et al., 2014). The correlations found in the present study support the use of a kinematic-driven STA model (Camomilla et al., 2015; De Rosario et al., 2013), although they were restricted to some of the translations and rotations of the marker-cluster.

The present study has some limitations. First, only one motor task (treadmill walking) was studied. Second, a marker-cluster made of all markers was analysed while combinations of multiple marker-clusters selected with different rationales (Barré et al., 2015; Grimpampi et al., 2013; Solav et al., 2016) have not been investigated. Third, the analysis was based on a modal description of the STA and the corresponding energy (i.e. a threshold of 80% of the STA energy was arbitrary set) but the propagation of the STA to the knee joint kinematics was not analysed. Finally, the correlation and cross-correlation between the amplitudes and the joint angles were limited to the knee flexion, while thigh and shank STA can be also related to hip and ankle kinematics, respectively (Camomilla et al., 2015). These correlation and cross-correlation were computed over the 15-second records whatever the number of steps was. The rationale for analysing the data with a fixed time window rather than cycle-by-cycle as performed in Barré et al. (2013) was that, in the present study, the amplitude was not plotted against time but against knee flexion and the minimum and maximum of this angle did not match with the heel-strike and

toe-off events.

5. Conclusion

The present study aimed at confirming the recent findings on the STA, which were focussed on the translations and rotations of the marker-cluster, with a large number of markers placed on the segments. With up to 40 markers placed on the segments, the translations, rotations, stretches and homotheties of the marker-cluster were almost all required to describe the STA, thus revealing more complex patterns of the STA than previously reported with marker-clusters made of 4 to 6 markers. Nevertheless, translations and rotations remained the main STA modes and the amplitudes of some of these modes where correlated to the knee flexion angle. These findings support the current re-orientation of STA compensation methods, from bone pose estimators which typically address the non-rigid components of the marker-cluster to kinematic-driven rigid-component STA models.

Conflict of interest statement

The authors declare no conflict of interest.

Acknowledgements

This work was partly supported the “Fondation de soutien à la recherche dans le domaine de l’othorpédie et traumatologie”. This work was performed within the framework of the LABEX PRIMES (ANR-11-LABX-0063) of Université de Lyon, within the program "Investissements d'Avenir" (ANR-11-IDEX-0007) operated by the French National Research Agency (ANR).

References

Akbarshahi, M., Schache, A.G., Fernandez, J.W., Baker, R., Banks, S., Pandy, M.G., 2010. Non-invasive assessment of soft-tissue artifact and its effect on knee joint kinematics during functional activity. J Biomech 43, 1292-1301.

Andersen, M.S., Damsgaard, M., Rasmussen, J., Ramsey, D.K., Benoit, D.L., 2012. A linear soft tissue artefact model for human movement analysis: proof of concept using in vivo data. Gait Posture 35, 606-611.

Andriacchi, T.P., Alexander, E.J., Toney, M.K., Dyrby, C., Sum, J., 1998. A point cluster method for in vivo motion analysis: applied to a study of knee kinematics. J Biomech Eng 120, 743-749.

Barré, A., Jolles, B.M., Theumann, N., Aminian, K., 2015. Soft tissue artifact distribution on lower limbs during treadmill gait: Influence of skin markers' location on cluster design. Journal of Biomechanics 48, 1965-1971.

Barré, A., Thiran, J.P., Jolles, B.M., Theumann, N., Aminian, K., 2013. Soft tissue artifact assessment during treadmill walking in subjects with total knee arthroplasty. IEEE Transactions on Biomedical Engineering 60, 3131-3140.

Benoit, D.L., Damsgaard, M., Andersen, M.S., 2015. Surface marker cluster translation, rotation, scaling and deformation: Their contribution to soft tissue artefact and impact on knee joint kinematics. Journal of Biomechanics 48, 2124-2129.

Bonci, T., Camomilla, V., Dumas, R., Chèze, L., Cappozzo, A., 2015. Rigid and non-rigid geometrical transformations of a marker-cluster and their impact on bone-pose estimation. Journal of Biomechanics 48, 4166-4172.

Camomilla, V., Bonci, T., Dumas, R., Chèze, L., Cappozzo, A., 2015. A model of the soft tissue artefact rigid component. Journal of Biomechanics 48, 1752-1759.

Cappello , A., Stagni, R., Fantozzi, S., Leardini, A., 2005. Soft tissue artifact compensation in knee kinematics by double anatomical landmark calibration: performance of a novel method during selected motor tasks. IEEE Transactions on Biomedical Engineering 52, 992-998.

Cappozzo, A., Catani, F., Leardini, A., Benedetti, M.G., Croce, U.D., 1996. Position and orientation in space of bones during movement: experimental artefacts. Clin Biomech (Bristol, Avon) 11, 90-100.

de Rosario, H., Page, A., Besa, A., Mata, V., Conejero, E., 2012. Kinematic description of soft tissue artifacts: quantifying rigid versus deformation components and their relation with bone motion. Medical & Biological Engineering & Computing 50, 1173-1181.

De Rosario, H., Page, A., Besa, A., Valera, A., 2013. Propagation of soft tissue artifacts to the center of rotation: A model for the correction of functional calibration techniques. J Biomech 46, 2619-2625.

Dumas, R., Camomilla, V., Bonci, T., Cheze, L., Cappozzo, A., 2014a. Generalized mathematical representation of the soft tissue artefact. Journal of Biomechanics 47, 476-481.

Dumas, R., Camomilla, V., Bonci, T., Cheze, L., Cappozzo, A., 2014b. A qualitative analysis of soft tissue artefact during running. Computer Methods in Biomechanics and Biomedical Engineering 17, 124-125.

Dumas, R., Camomilla, V., Bonci, T., Chèze, L., Cappozzo, A., 2015. What Portion of the Soft Tissue Artefact Requires Compensation When Estimating Joint Kinematics? Journal of Biomechanical Engineering 137, 064502-064501 - 064502-064505.

Dumas, R., Cheze, L., 2009. Soft tissue artifact compensation by linear 3D interpolation and approximation methods. J Biomech 42, 2214-2217.

Fiorentino, N.M., Atkins, P.R., Kutschke, M.J., Foreman, K.B., Anderson, A.E., 2016. In-vivo quantification of dynamic hip joint center errors and soft tissue artifact. Gait & posture 50, 246-251.

Grimpampi, E., Camomilla, V., Cereatti, A., de Leva, P., Cappozzo, A., 2013. Metrics for describing soft-tissue artefact and its effect on pose, size, and shape of marker clusters. IEEE Transactions on Biomedical Engineering, 10.1109/TBME.2013.2279636.

Hara, R., Sangeux, M., Baker, R., McGinley, J., 2014. Quantification of pelvic soft tissue artifact in multiple static positions. Gait & posture 39, 712-717.

Heller, M.O., Kratzenstein, S., Ehrig, R.M., Wassilew, G., Duda, G.N., Taylor, W.R., 2011. The weighted optimal common shape technique improves identification of the hip joint center of rotation in vivo. Journal of orthopaedic research : official publication of the Orthopaedic Research Society 29, 1470-1475.

Leardini, A., Chiari, L., Della Croce, U., Cappozzo, A., 2005. Human movement analysis using stereophotogrammetry. Part 3. Soft tissue artifact assessment and compensation. Gait Posture 21, 212-225.

Peters, A., Galna, B., Sangeux, M., Morris, M., Baker, R., 2010. Quantification of soft tissue artifact in lower limb human motion analysis: a systematic review. Gait Posture 31, 1-8.

Richard, V., Camomilla, V., Cheze, L., Cappozzo, A., Dumas, R., 2012. Feasibility of incorporating a soft tissue artefact model in multi-body optimisation. Computer Methods in Biomechanics and Biomedical Engineering 15, 194-196.

Richard, V., Cappozzo, A., Dumas, R., 2017. Comparative assessment of knee joint models used in multi-body kinematics optimisation for soft tissue artefact compensation. Journal of Biomechanics, in press.

Sangeux, M., Marin, F., Charleux, F., Durselen, L., Ho Ba Tho, M.C., 2006. Quantification of the 3D relative movement of external marker sets vs. bones based on magnetic resonance imaging. Clin Biomech (Bristol, Avon) 21, 984-991.

Soderkvist, I., Wedin, P.A., 1993. Determining the movements of the skeleton using well-configured markers. J Biomech 26, 1473-1477.

Solav, D., Rubin, M.B., Cereatti, A., Camomilla, V., Wolf, A., 2016. Bone Pose Estimation in the Presence of Soft Tissue Artifact Using Triangular Cosserat Point Elements. Annals of Biomedical Engineering 44, 1181-1190.

Figure and table captions

Table 1: Occurrences (among the 19 subjects) for the shank of the geometrical transformations of the marker-cluster in the ranked modes (ordered according to their energy λ_1^l). X-axis is medial-lateral pointing to the left, the Y-axis is proximal-distal pointing upward, and the Z-axis is anterior-posterior pointing frontward.

Table 2: Occurrences (among of the 19 subjects) for the thigh of the geometrical transformations of the marker-cluster in the ranked modes (ordered according to their energy λ_2^l). X-axis is medial-lateral pointing to the left, the Y-axis is proximal-distal pointing upward, and the Z-axis is anterior-posterior pointing frontward.

Figure 1: Modal amplitudes plotted against the knee flexion angles for the 15-second records of the 19 subjects (one colour by subject). (A) Translation along the proximal-distal (Y) axis for the shank. (B) Stretch about the proximal-distal (Y) axis for the shank. (C) Homothety about the proximal-distal (Y) axis for the shank. (D) Translation along the proximal-distal (Y) axis for the thigh. (E) Rotation about the medial-lateral (X) axis for the thigh. Heel strike and toe-off events are represented by circles and squares, respectively.

Table 1

		Rank number											
		#1	#2	#3	#4	#5	#6	#7	#8	#9	#10	#11	#12
Translation	**X**		1	4	3	2	3	3		2	1		
	Y	7	4	2	1	4		1					
	Z	8	6	1	3	1							
Rotation	**X**		2	4	5	2	1	4	1				
	Y	2	2	4	3	4	1	1	2				
	Z				2		5	1	6	3	1		1
Stretch	**X**		1		1		2		3	2	4	4	2
	Y	1	1	3		2	4	4	1		1	1	
	Z					1	1	1	3	4	4	4	1
Homothety	**X**					1		1		3	2	5	6
	Y		1		1	2	2	3	2		3		5
	Z	1	1	1					1	5	2	4	2
Total of occurrences (number of subjects with $r_1 \geq$ rank number)		19	19	19	19	19	19	19	19	19	18	18	17

Table 2

		Rank number											
		#1	#2	#3	#4	#5	#6	#7	#8	#9	#10	#11	#12
Translation	**X**		2	3	5	1	2				1		
	Y	14	5										
	Z		3	7	5	4							
Rotation	**X**	3	7	3	1	2	2						
	Y	2	1	5	5	2	2						
	Z						1	4	1	1	1		
Stretch	**X**			1	2	5	2	2	1		1		
	Y		1		1	1	2	2	2				1
	Z					1	1	1	1			2	
Homothety	**X**								1	1			2
	Y									2	1	1	
	Z					1	1	1		1	1	1	1
Total of occurrences (number of subjects with $r_2 \geq$ rank number)		19	19	19	19	17	13	10	6	5	5	4	4